ISSN (Print) : 0974-6846
ISSN (Online) : 0974-5645

INDIAN JOURNAL OF SCIENCE AND TECHNOLOGY
January 2020, Vol 13(02), 161 – 192
DOI: 10.17485/ijst/2020/v13i02/148492,

Characterization of Outer Membrane Vesicles from *Fusobacterium nucleatum*

Raafat Munshi*

King Abdulaziz University Hospital, Jeddah, Saudi Arabia

Article Type: Article

Article Citation: Raafat Munshi. Characterization of outer membrane vesicles from Fusobacterium nucleatum *Indian Journal of Science and Technology*. 2020; 13(02), 161-192. DOI: 10.17485/ijst/2020/v013i02/148492

Received date: October 30, 2019

Accepted date: November 13, 2019

***Author for correspondence:** Raafat Munshi raafat.munshi@gmail.com King Abdulaziz University Hospital, Jeddah, Saudi Arabia

Abstract

Background/objectives: *Fusobacterium nucleatum* is an oral pathogen and is associated with the development of colorectal cancer (CRC). This study is to evaluate the ability of outer membrane vesicles (OMV) from *F. nucleatum* to modulate cellular responses in colonic cells. **Methodology:** Here we show that infection of colonic epithelial cells with *F. nucleatum* and its OMV induce pro-inflammatory chemokine and cytokine production and promote an EMT-like pheno- and genotypes *in vitro* as demonstrated by suppression of E-cadherin and up-regulation of several mesenchymal markers. *F. nucleatum* and its OMV modulate the barrier function of intestinal monolayers, a process likely related to their demonstrated ability to degrade E-cadherin and suppress its expression. **Findings**: Analysis of the OMV proteome by mass spectrometry demonstrates that they harbor the known virulence factors that appear to be enriched with proteolytic activity. **Novelty/contribution**: Taken together, these data indicate that *F. nucleatum* OMV have the potential to contribute to disease progression in the context of CRC.

Keywords: Outer Membrane Vesicles, *Fusobacterium nucleatum*, Colorectal Cancer, Protease.

1. Introduction

In colorectal cancer (CRC), mutations in the APC/Wnt pathway in colonic epithelial stem cells lead to the formation of adenomatous lesions [1]. Current evidence indicates a role for the microbiota in CRC with specific species/genera and polymicrobial signatures associated with CRC adenomas and tumors [2–4]. Others have proposed a role for concomitant reduction of the anti-inflammatory butyrate-producing commensals (e.g., Roseburia, Lachnospiraceae) in the pathogenesis of CRC [3].

Consistent demonstration, however, of *Fusobacterium nucleatum* enrichment at colonic adenoma and tumor sites [5–10] has revealed that CRC patients with low abundance of *F. nucleatum* have prolonged survival compared to those with moderate to high abundance [9,11].

Coupled with its ability to evade the immune response by inhibiting NK cell cytotoxicity and tumor killing [12], this microbe is now being considered as a marker for CRC [13]. *F. nucleatum* adheres to and invades epithelial cells via the adhesin FadA [14] which engages with host E-cadherin resulting in nuclear translocation of β-catenin and activation of the Wnt pathway [6,14]. Pre-clinical studies show that *F. nucleatum* promotes colonic tumorigenesis. However, as *F. nucleatum* is considered a "bridging" biofilm-promoting organism in the oral cavity, disease progression may be influenced by mechanisms shared between bacterial species rather than just *F. nucleatum* [15].

With regard to pathogen–host interactions, we were interested to evaluate the role of *F. nucleatum* outer membrane vesicles (OMV) as potential modulators of host cellular responses as OMV can mimic the activities of pathogenic and non-pathogenic parental bacteria. OMVs are closed proteo-liposomes composed of LPS, lipids, lipoproteins/peptides, porins/receptors, adhesins, and peptidoglycan. Functions attributed to OMVs include quorum sensing, horizontal transfer of virulence factors, co-aggregation, and biofilm formation in addition to having significant roles in disease.

Here we report that *F. nucleatum* OMV induce colonic epithelial cell proliferation; the release of pro-inflammatory and immune-regulatory cytokines; degrade E-cadherin and downregulate CDH1; disrupt barrier integrity of epithelial monolayers; initiate a pro-inflammatory milieu and induce morphological changes consistent with a mesenchymal phenotype/genotype. Taken together, these data suggest that *F. nucleatum* OMV are potent modulators of colonic epithelial cell function and may contribute to colonic pathology both at the site of colonization and distally.

2. Materials and Methods

2.1. Bacterial Strains, Cell Lines, and Culture Conditions

Fusobacterium nucleatum nucleatum (ATCC 25586), and the subspecies polymorphum (ATCC 10953) and vincentii (ATCC 49256) were purchased from the ATCC culture collection (ATCC, LGC, UK). All strains were grown at 37 °C under anaerobic conditions using the AnaeroGen atmosphere generating system (ThermoScientific). Fusobacteria were thawed from frozen stock (BHI containing 50% (v/v) glycerol) and grown on Columbia blood agar plates (Columbia agar base, Oxoid) supplemented with 7% (v/v) defibrinated horse blood. For broth culture, Fusobacteria were grown in brain heart infusion broth which was pre-reduced for at least 24 h under anaerobic conditions before use. Different preparations of the bacterium were routinely Gram stained (Sigma) and observed under oil immersion (100×) to ensure purity and to check morphology and integrity. The number of bacteria was quantified as described [16].

Colonic cancer cell lines were cultured in MEM supplemented with l-glutamine (Caco-2: ATCC HTP-37), Dulbecco's MEM/Hams F13 medium (T84: ATCC CCL-248) or RPMI (SW 480 and 620: ATCC CCL-228 and -227, respectively), LoVo (ATCC CCL-229)) containing 10% (v/v) foetal calf serum, penicillin (100 U/ml), and streptomycin (100 μg/ml). SW480 cells are a primary adenocarcinoma, non-metastatic, cell line and its

lymph node metastasis equivalent [17]. T84, Caco-2, and LoVo cells are adherent human epithelial colon carcinoma cell lines which form polarized/differentiated monolayers on semi-permeable supports *in vitro*.

2.2. Outer Membrane Vesicle Isolation and Proteomic Composition

OMV were purified from broth cultures of Fusobacteria species essentially as described previously [18]. The bacteria were cultured (10 × 50 ml) for 48–72 h prior to OMV recovery. OMV were examined by transmission electron microscopy to determine purity and size heterogeneity. The OMVs were mounted onto carbon-colloidal-coated mesh grids and let settle for 60 s. Residual non-adherent OMV were removed using filter paper wicks. The samples were left to air dry and stained using aqueous uranyl acetate (1%, v/v).
Purified OMV were subjected to SDS-PAGE and the resulting Colloidal Coomassie G-250 stained gel was cut into 10 pieces prior to in-gel digestion, using a ProGest Investigator in-gel digestion robot (Genomic Solutions, Ann Arbor, MI) using standard protocols at the BMS Mass Spectroscopy facility, University of St Andrews.

2.3. Cell Proliferation

Epithelial cells were seeded in 96-well plates at 2 × 104 cells/well. Cells were either left untreated or stimulated with *F. nucleatum* (MOI: 0–500:1) or different amounts of OMV (0–50 µg/ml). Quadruplicate assays were undertaken with an additional well used to determine cell viability using the Trypan blue exclusion assay. After selected time points Cell Titre One reagent (Promega) was added and the absorbance (490 nm) read using Wallac Victor2 plate reader.

2.4. Trans-epithelial Electrical Resistance (TEER)

Caco-2 or T-84 colonic epithelial cells were seeded in 12-well 0.4 µm 6.5 mm PET membrane inserts (uncoated polyethylene terephthalate plastic trace-etched membranes, Falcon, Beckton Dickinson) at 4–5 × 105 cells/ml. The cells were fed both apically and basally every 24–48 h and cultured in a humidified incubator at 37 °C, 5% CO2. The TEER was measured using an EVOM epithelial voltammeter apparatus (World Precision Instruments). Typically, fully polarized and differentiated monolayers took 10–14 days to form after which time the monolayers were exposed to bacteria/OMV and the resistance monitored over time. Triplicate or quadruplicate wells for each condition were used routinely.

3. Immunofluorescence Imaging

Following treatment and incubation of cells as required, the cells were washed with PBS (×2) prior to fixation with paraformaldehyde (4%, w/v) in PBS for 15 min followed by

PBS washing (×2). Cells were then permeabalized with Triton X-100 (0.3%, v/v) in PBS for 5 min at room temperature (RT), followed by blocking with bovine serum albumin (BSA; 3%, w/v) in PBS at RT for 1 h. Hoechst (1:2000) and phalloidin-TRITC (1:500) were added to the blocking buffer. Following washing, the cells were incubated with primary antibody diluted in BSA (3%, w/v) in PBS and incubated overnight at 4 °C. The cells were washed with PBS (×3), followed by incubation with the appropriate secondary antibody conjugated to Alexa 488 or Alexa 594 (Invitrogen) for 1 h at RT. Images were captured using an inverted light microscope (Nikon, Eclipse TE-300).

3.1. SDS-PAGE, Zymography, and WESTERN Blotting

Protein solutions were quantified using the BCA (Pierce) protein assay or with a Nanodrop 8000 UV–Vis spectrophotometer and electrophoresed on gradient (5–20%) or uniform concentration (12.5%) acrylamide gels using standard conditions.

Zymography was performed using gradient acrylamide gels copolymerized with bovine gelatin (Sigma; 0.05–0.1%, w/v). Non-reducing sample buffer was used to solubilize samples without heat denaturation. Gels were electrophoresed at constant current (25 mA/gel). Following electrophoresis, the gels were washed for 1 h in Triton X-100 (2.5%, v/v) with gentle shaking, to remove excess SDS, followed by static incubation for approximately 24 h (37 °C) in 25 mM Tris buffer (pH 7.2), supplemented with 5 mM CaCl2. Gels were then stained with Coomassie blue (R250) for at least 1 h followed by de-staining in methanol (30%, v/v) and acetic acid (10%, v/v). Zones of proteolysis were visualized as clear areas against a light or dark blue background, depending on the extent of destaining required.

3.2. Western Blotting

Proteins (25–50 µg/lane) were transferred (1 mA/cm2 for 1 h) to polyvinylidene difluoride membrane (Roth) using a semi-dry blotting apparatus (Atto). Blots were blocked with non-fat dry milk (5%, w/v) or BSA (3%, w/v), in PBS, followed by incubation with the appropriate primary antibody overnight at 4 °C. Following washing with PBS containing Tween-20 (0.05%, v/v), blots were incubated with secondary antibody for 1 h at RT, washed and developed using enhanced chemiluminescence. Densitometry of gels/blots was performed using ImageJ software (NIH) with expression levels of proteins normalized to an appropriate loading control.

3.3. LPS Purification

The method for LPS isolation from *F. nucleatum* was performed essentially as described in Ref. [19] and the sliver staining protocol described in Ref. [20] was used to assess purity.

Primary antibodies. The following antibodies were used: Anti-ZEB-1 (Novus Biologicals, NBP1-88845 or NBP1-05987); Anti-E-cadherin (BD Transduction: 610182); Anti-PCNA (Novus Biologicals: NB500-106H); Anti-tubulin (Sigma: T6199); Anti-STAT-3 (Cell Signalling: D3Z2G); and Anti-p-STAT-3 (Cell Signalling: D3A7).

3.4. Determination of Cytokine/Chemokine Production

The amount of IL-8 secreted by colonic cells in response to various treatments was determined by ELISA (R&D Duoset) according to the manufacturer's instructions.

3.5. qPCR

Primers used for RT-PCR are shown in Table S1. All primers were predesigned KiCqStart SYBR Green RT-qPCR Primers (Sigma). cDNA was obtained using the SensiFAST cDNA Synthesis Kit (Bioline) according to the manufacturer's instructions. The quantity of extracted cDNA was evaluated using a Nanodrop 8000. The qPCR assay was performed using the sensiFAST SYBR No-ROX Kit (Bioline) as recommended. The following amplification conditions were used on the Illumina Eco RT-PCR System: (i) pre-amplification cycle for 15 min at 95 °C, 40 amplification cycles for 1 min at 95 °C, 1 min at 55 °C and 1 min at 72 °C (ii) end-amplification cycle for 15 s at 95 °C, 15 s at 55 °C,

TABLE S1. Primers used for RT-PCR

Primer	Forward sequence	Reverse sequence
GAPDH	ACAGTTGCCATGTAGACC	TTTTTGGTTGAGCACAGG
IL-8	GTTTTTGAAGAGGGCTGAG	TTTGCTTGAAGTTTCACTGG
CXCL-1	ATGCTGAACAGTGACAAATC	TCTTCTGTTCCTATAAGGGC
TNF-α	AGGCAGTCAGATCATCTTC	TTATCTCTCAGCTCCACG
IL-1 β	CTAAACAGATGAAGTGCTCC	GGTCATTCTCCTGGAAGG
IL-6	GCAGAAAAAGGCAAAGAATC	CTACATTTGCCGAAGAGC
CCL-20	TATATTGTGCGTCTCCTCAG	GCTATGTCCAATTCCATTCC
MMP-1	AAAGGGAATAAGTACTGGGC	CAGTGTTTTCCTCAGAAAGAG
MMP-2	GTGATCTTGACCAGAATACC	GCCAATGATCCTGTATGTG
MMP-9	AAGGATGGGAAGTACTGG	GCCCAGAGAAGAAGAAAAG
MMP-10	AGCGGACAAATACTGGAG	GTGATGATCCACTGAAGAAG
MMP-13	AGGCTACAACTTGTTTCTTG	AGGTGTAGATAGGAAACATGAG
BMP-1	GATGTGAAAAAGGACTATGGC	AATCTCAAAGGACTGGAATG
FN-1	CCATAGCTGAGAAGTGTTTTG	CAAGTACAATCTACCATCATCC
ITGA-5	AAGCTTGGATTCTTCAAACG	TCCTTTTCAGTAGAATGAGGG
CDH-1	CCGAGAGCTACACGTTC	TCTTCAAAATTCACTCTGCC
CDH-2	ACATATGTGATGACCGTAAC	TTTTTCTCGATCAAGTCCAG
Snal-1	CTCTAATCCAGAGTTTACCTTC	GACAGAGTCCCAGATGAG
Snal-2	CAGTGATTATTTCCCCGTATC	CCCCAAAGATGAGGAGTATC
Snal-3	TCCTTCCTGGTGAAAACG	CACCATTGATTTCTCTCTGC
ZEB-1	AAAGATGATGAATGCGAGTC	TCCATTTTCATCATGACCAC
TWIST-1	CTAGATGTCATTGTTTCCAGAG	CCCTGTTTCTTTGAATTTGG
Vimentin	GGAAACTAATCTGGATTCACTC	CATCTCTAGTTTCAACCGTC
NF-κβ 1	GACAACTATGAGGTCTCTGG	ATCACTTCAATTGCTTCGG
NF-κβ 2	TGAAGATTTCTCGAATGGAC	ACCTCAATGTCATCTTTCTG
SOCS-3	CCTATTACATCTACTCCGGG	ACTTTCTCATAGGAGTCCAG
SPHK-1	TTCCTTGAACCATTATGCTG	GATACTTCTCACTCTCTAGGTC
PTGS-2	AAGCAGGCTAATACTGATAGG	TGTTGAAAAGTAGTTCTGGG
Wnt-7 α	AAAGATCCTGGAGGAGAAC	TGATCTTCAGGAAGGTGG
Wnt-7 β	GCAGGAAGGTTCTAGAGG	GTTGTACTTCTCCTTCAGC
Wnt-9 α	GGTGTGAAGGTGATCAAG	TGCCGTCTCATACTTGTG
MYC	TGAGGAGGAACAAGAAGATG	ATCCAGACTCTGACCTTTTG

and 15 s at 95 °C. All reactions were run in duplicate or triplicate with non-template and reverse transcriptase controls and normalized to GAPDH expression. Ct values were obtained during the exponential amplification phase using EcoStudy software (Illumina) and exported into Microsoft Excel for further analysis.

3.6. Statistical Analyses

Significant differences were determined by either applying the Student's *t*-test or analysis of variance (ANOVA), where appropriate.

4. Results

4.1. Isolation and Proteomic Analysis of *F. nucleatum* OMV

OMV isolated from the supernatant of broth grown *F. nucleatum* were 20–200 nm in diameter and free from intact cells and/or cellular debris (Figure 1A). Preparations of OMV contained two types of vesicles, single membrane and bi-layered species. The latter type (outer–inner MV) are released by other bacteria and contain both the inner cytoplasmic and outer membrane proteins [21] and likely account for the presence of cytoplasmic components frequently observed associated with OMV.

Proteomic analysis of *F. nucleatum* OMV identified 367 proteins (Tables S2–S6) and the predicted subcellular distribution of the constituents, determined using pSortB, is shown in Figure 1B.

TABLE S2. Cytoplasmic proteins (193, 52.32%) identified in F. nucleatum OMV

Accession number[a]	Protein score[b]	% Coverage[c]	Number of peptide matches[d]	Description
gi|19704946	205	42.8	16	50S ribosomal protein L15P
gi|19705258	112	19.4	3	Hypothetical Protein FN1956
gi|19703929	131	43.3	18	(3R)-hydroxymyristoyl-ACP dehydratase
gi|19705272	130	33.5	11	4-amino-4-deoxychorismate lyase
gi|19705330	481	54.5	46	50S ribosomal protein L1
gi|19705329	153	47.1	12	50S ribosomal protein L10P
gi|19704452	139	42.3	15	50S ribosomal protein L21P
gi|19704636	102	25	23	ABC transporter ATP-binding protein
gi|19703509	946	69.4	45	Anhydro-N-acetylmuramyl-tripeptide amidase
gi|19703677	207	25.5	14	Aspartate/aromatic aminotransferase
gi|19703545	329	64.9	18	Biotin carboxyl carrier protein of glutaconyl-COA decarboxylase

gi|19704783	233	33.3	17	Cell division protein FtsZ
gi|19705415	124	16.6	15	DNA gyrase subunit A
gi|19703626	79	4.2	5	DNA polymerase III subunit alpha
gi|19704618	105	29.8	17	DNA-directed RNA polymerase subunit alpha
gi|19704887	3191	84.5	157	Elongation factor Tu
gi|19703700	156	31.8	13	F0F1 ATP synthase subunit beta
gi|19705372	175	14.7	9	Formatetetrahydrofolate ligase
gi|19703370	446	52.6	22	Hypothetical protein FN0018
gi|19704123	100	58.3	13	Hypothetical protein FN0788
gi|19704424	138	31	10	Hypothetical protein FN1089
gi|19704860	249	61	23	Hypothetical protein FN1528
gi|19704939	384	53.1	27	Hypothetical protein FN1618
gi|19705040	1407	76.2	99	Hypothetical protein FN1719
gi|19705282	131	26.2	12	Hypothetical protein FN1986
gi|19705408	234	73.1	29	Hypothetical protein FN2118
gi|19703633	76	34.9	8	Hypoxanthine-guanine phosphoribosyltransferase
gi|19704566	141	37	19	Inosine-5′-monophosphate dehydrogenase
gi|19705114	92	17.7	6	Iron/zinc/copper-binding protein
gi|19704871	155	19.1	5	Iron-sulfur cluster-binding protein
gi|19703419	84	10.3	10	Isoleucyl-tRNA synthetase
gi|19704504	94	18.6	7	L-lactate dehydrogenase
gi|19705000	121	31.4	11	LPS biosynthesis protein WbpG
gi|19704441	96	12.7	4	L-serine dehydratase
gi|19703801	106	22.5	15	lysyl-tRNA synthetase
gi|19703494	571	43.8	30	Malonyl-coa-[acyl-carrier-protein] transacylase
gi|19704917	189	30.8	16	Nitrogen fixation iron-sulphur protein RNFC
gi|19703769	85	13.7	4	Orotate phosphoribosyltransferase
gi|19704711	132	29.2	16	Oxaloacetate decarboxylase
gi|19705105	215	33.7	30	Peptidyl-prolyl cis-trans isomerase
gi|19705412	607	44	63	Phenylalanyl-tRNA synthetase beta chain
gi|19704051	94	15	7	Phophatidylinositol-4-phosphate 5-kinase
gi|19704507	1046	52.8	75	Phosphate acetyltransferase
gi|19703989	245	54	26	Phosphoglycerate kinase
gi|19704064	156	44.3	15	Phosphoglycerate mutase
gi|19704323	90	14.8	6	Phosphoribosylaminoimidazole-succinocarboxamide synthase

gi|492611374	355	48.5	30	Phosphotransacetylase
gi|19705045	87	17	4	Potassium uptake protein KtrA
gi|19704305	107	32	8	Precorrin-8X methylmutase
gi|19705039	271	41.2	72	Preprotein translocase subunit SecA
gi|19704888	487	38.5	51	Elongation factor G
gi|19704622	102	22	2	Protein translation initiation factor 1
gi|492614315	117	33.5	8	PTS glucose transporter subunit IIA
gi|19704250	254	57.3	32	PTS system, N-acetylglucosamine-specific IIA component
gi|19704795	98	36.4	9	Pyridoxal biosynthesis lyase PdxS
gi|19704505	689	27.9	59	Pyruvate-flavodoxin oxidoreductase
gi|19705288	86	16.8	7	Ribose-phosphate pyrophosphokinase
gi|19704944	125	12.6	4	Ribosome recycling factor (RRF)
gi|19704912	168	25.2	8	RNFB-related protein
gi|19704093	124	39.9	22	Rod shape-determining protein MreB
gi|19704013	320	40	18	Ser/Thr protein kinase
gi|19713538	150	32.3	14	Seryl-tRNA synthetase
gi|19703829	189	35	16	Short chain dehydrogenase
gi|19703796	257	60.2	23	Sigma(54) modulation protein
gi|19705007	434	40.2	34	Spore coat polysaccharide biosynthesis protein spsF
gi|19704339	81	22.3	6	TetR family transcriptional regulator
gi|19705322	243	30.3	14	Thiamine biosynthesis lipoprotein apbE
gi|19703445	230	69.9	12	Thioredoxin FN0093
gi|19704743	179	21.5	5	Threonine dehydratase
gi|19703946	98	39.6	8	Threonyl-tRNA synthetase
gi|19703640	240	40.8	11	Transketolase
gi|19705316	372	29.7	27	Translation initiation factor IF-2
gi|19703670	77	29.8	10	Translation initiation factor IF-3
gi|19705269	164	21.9	7	Translation initiation inhibitor
gi|19704701	118	47	13	Triosephosphate isomerase
gi|19705044	143	25	18	tRNA uridine 5-carboxymethylaminomethyl modification enzyme GidA
gi|19705248	94	17.2	9	Tryptophanase
gi|19705010	123	45.2	26	UDP-4-dehydro-6-deoxy-2-acetamido-D-glucose 4-reductase
gi|19703818	198	42.1	19	Uracil phosphoribosyltransferase

gi|19704943	78	31.8	12	Uridylate kinase
gi|19704127	120	18.4	13	Urocanate hydratase
gi|19703623	94	17	5	Xaa-His dipeptidase
gi|19704614	102	16.6	7	Zinc metallohydrolase
gi|19705172	98	28.7	7	Zn-dependent alcohol dehydrogenase and related dehydrogenase
gi|19703553	826	52.9	39	(R)-2-hydroxyglutaryl-CoA dehydratase beta-subunit
gi|19704868	163	24.2	12	(S)-2-hydroxy-acid oxidase chain D
gi|19704796	156	15.3	9	1-deoxy-D-xylulose-5-phosphate synthase
gi|19704772	100	21.3	7	1-phosphofructokinase
gi|19704851	173	28.6	8	23S rRNA methyltransferase
gi|19704840	120	43.6	26	3,4-dihydroxy-2-butanone-4-phosphate synthase
gi|19704967	322	62.1	25	30S ribosomal protein S10P
gi|19704724	276	59.8	16	30S ribosomal protein S16P
gi|19704941	265	47.4	33	30S ribosomal protein S2
gi|19704960	234	52.1	22	30S ribosomal protein S3P
gi|19704951	592	53.8	39	30S ribosomal protein S8P
gi|19705086	291	24.2	38	4-hydroxy-3-methylbut-2-enyl diphosphate reductase/
gi|19704420	89	30.8	7	4-methyl-5(B-hydroxyethyl)-thiazole monophosphate biosynthesis enzyme
gi|19704956	506	50.8	24	50S ribosomal protein L14P
gi|19703772	470	61.2	46	50S ribosomal protein L19
gi|19703668	323	40.5	21	50S ribosomal protein L20
gi|19704950	284	58.8	33	50S ribosomal protein L6
gi|19705133	151	37.6	13	50S ribosomal protein L9P
gi|19703830	403	49.5	25	acetyl-CoA acetyltransferase
gi|19705279	146	27.7	8	Alkyl hydroperoxide reductase C22 protein
gi|19703392	148	27.5	13	Asparaginyl-tRNA synthetase
gi|19705161	812	65.4	46	Butyrate-acetoacetate CoA-transferase subunit B
gi|19703464	316	31.1	22	Chaperone protein DnaK
gi|19704151	163	66.4	17	Dehydrogenase
gi|19705185	86	41.1	12	Dihydropteridine reductase
gi|19703822	224	41.4	20	D-lactate dehydrogenase
gi|19705416	131	18.9	16	DNA gyrase subunit B
gi|19705326	109	6.8	9	DNA-directed RNA polymerase subunit beta'

gi|19704865	386	45.5	28	Electron transfer flavoprotein subunit alpha
gi|19705083	370	45.6	25	Enolase
gi|19703607	1516	52.2	153	Formate acetyltransferase
gi|19703667	999	74.9	68	Fructose-1,6-bisphosphate aldolase
gi|19705008	151	40.4	16	Gluconate 5-dehydrogenase
gi|19703547	130	31.2	15	Glutaconate coa-transferase subunit A
gi|19704729	90	25	3	Glutaminase
gi|19704192	308	29.3	30	Glycogen phosphorylase
gi|19703422	125	37.3	57	Glycyl-trna synthetase beta chain
gi|19703383	102	21	5	Hypothetical Protein FN0031
gi|19703454	243	55.7	12	Hypothetical Protein FN0106
gi|19703674	124	16.7	6	Hypothetical Protein FN0331
gi|19703891	165	39.3	7	Hypothetical Protein FN0556
gi|19704023	246	41.8	9	Hypothetical Protein FN0688
gi|19704155	223	35.9	23	Mercuric Reductase
gi|19704603	110	10.8	6	Methionyl-trna synthetase
gi|19704036	80	12.2	7	Methyltransferase
gi|496072988	191	27.6	21	Molecular chaperone GroEL
gi|19704011	189	64.4	7	Molecular chaperone GroES
gi|19704060	196	45.7	13	molybdopterin biosynthesis MoeB protein
gi|19705005	208	34.2	12	N-acetylneuraminate synthase
gi|19704414	96	27.1	12	Neutrophil-activating protein A
gi|19704889	236	78.8	25	30S ribosomal protein S7
gi|19704355	149	50	19	3-hydroxybutyryl-coa dehydratase
gi|19705331	661	63.1	38	50S ribosomal protein L11P
gi|19703672	436	69.4	28	50S ribosomal protein L13
gi|19704617	100	45.7	28	50S ribosomal protein L17P
gi|19704961	155	39.6	11	50S ribosomal protein L22P
gi|19704966	572	44.5	30	50S ribosomal protein L3
gi|19704506	254	35.7	21	Acetate kinase
gi|19704638	337	44.3	17	Adenosylcobalamin-dependent diol dehydratase gamma subunit
gi|19704784	126	23	11	Cell division protein ftsa
gi|19705246	126	15.5	17	ClpB protein
gi|19704932	86	13.8	2	Competence protein
gi|19703410	243	45.1	33	Cysteine desulfhydrase
gi|19704555	486	40.8	36	Cysteine synthase
gi|19705146	78	36.1	12	Dihydroxyacetone kinase

gi|19703888	127	24.9	22	D-serine dehydratase
gi|161485655	576	60.3	40	Elongation factor Ts
gi|19703548	214	49.1	19	Glutaconate coa-transferase subunit B
gi|19703987	178	31.9	27	Glyceraldehyde 3-phosphate dehydrogenase
gi|19703666	102	21.3	12	Heat shock protein 90
gi|19704397	90	23.5	8	Hydrolase
gi|19703661	380	70.9	32	Hypothetical protein FN0316
gi|19703794	160	23.8	6	Hypothetical protein FN0459
gi|19704181	470	56.2	40	Hypothetical protein FN0846
gi|19704259	95	12.1	3	Hypothetical protein FN0924
gi|19704948	197	51.8	22	30S ribosomal protein S5P
gi|19704965	368	38.3	31	50S ribosomal protein L4
gi|19705162	864	66.8	60	Acetoacetate:butyrate/acetate coenzyme A transferase
gi|19704633	134	64	15	Adenylate kinase
gi|19703644	121	22	11	Aspartyl-trna synthetase
gi|19704715	99	12.6	6	Citrate lyase beta chain
gi|19703592	684	68.1	45	Cytoplasmic protein
gi|19703911	108	17.1	5	D-amino acid dehydrogenase large subunit
gi|19704284	127	8.4	11	DNA helicase
gi|19704055	106	23.5	7	Elongation factor P
gi|19703519	95	26.1	7	Enoyl-[acyl-carrier-protein] reductase
gi|19704074	99	32.1	8	Formiminotetrahydrofolate cyclodeaminase
gi|492612068	696	56.7	54	Glutamate dehydrogenase
gi|19704076	120	33.3	12	Glutamate formiminotransferase
gi|19705283	99	19.4	7	GntR family transcriptional regulator
gi|19704158	137	21.5	14	GTP-binding protein hflX
gi|19704816	168	26.5	7	Hypothetical protein FN1484
gi|19703947	106	36.7	7	Hypothetical protein FN0612
gi|19704311	114	23.6	8	Hypothetical protein FN0976
gi|19704619	285	62.1	34	30S ribosomal protein S4
gi|19704953	392	60.1	37	50S ribosomal protein L5
gi|19704656	594	36.7	41	Acetoacetate metabolism regulatory protein atoC
gi|19704118	303	38.3	30	Acyl-coa dehydrogenase
gi|19705363	173	33.3	11	Adenine phosphoribosyltransferase

gi|19705019	253	30.9	17	dTDP-4-dehydrorhamnose reductase
gi|19704119	806	56.5	49	Electron transfer flavoprotein subunit beta
gi|19703787	271	29.2	24	Glucosamine--fructose-6-phosphate aminotransferase [isomerizing]
gi|19704881	191	47.6	20	Hypothetical protein FN1549
gi|19704963	281	43.5	19	50S ribosomal protein L2
gi|19703702	132	22.8	14	F0F1 ATP synthase subunit alpha
gi|19703594	127	42	8	Hypothetical protein FN0249
gi|19705178	190	54.5	9	Bis(5′-nucleosyl)-tetraphosphatase
gi|19703549	585	35.6	50	Glutaconyl-coa decarboxylase A subunit
gi|19703914	2000	46.9	143	Cytoplasmic protein

[a]**Accession number:** a unique identifier assigned to the protein by FASTA database.
[b]**Protein score:** the protein score is the sum of the highest ions score for each distinct sequence.
[c]**% Coverage:** The percentage of all the amino acids in the protein sequence that were covered by identified peptides detected in the sample, It is calculated from the length and the set of peptides assigned to the protein.
[d]**Number of peptide matches**: The number of distinct peptide sequences in the protein group.

TABLE S3. Cytoplasmic membrane proteins (32, 8.72%) identified in the proteome of F. nucleatum OMV

Accession number	Protein score	% Coverage	Number of peptide matches	Description
gi|19704586	84	5.8	2	High-affinity iron permease
gi|19704003	149	39.1	16	High-affinity zinc uptake system protein znua precursor
gi|19703356	158	20.5	11	Inner membrane protein
gi|19703718	151	17.3	8	Iron ABC transporter ATP-binding protein sfuC
gi|19704697	111	14.6	3	Peptide ABC transporter ATP-binding protein
gi|19704540	404	46.8	36	Protease FN1205
gi|19704606	121	13.3	14	Protease IV FN1271
gi|19703684	130	7.7	3	Transport protein FN0341
gi|19704462	230	20.5	15	Hypothetical protein FN1127
gi|19705281	164	19.4	10	Hypothetical protein FN1985
gi|19704202	78	20.2	21	Long-chain-fatty-acid-Coa ligase
gi|19705321	255	15.9	14	Membrane-bound proton-translocating pyrophosphatase
gi|19704863	116	17.6	6	Negative regulator of murein hydrolase
gi|19704034	78	14.1	5	Protein translocase subunit SecD

gi|19704670	138	40.4	9	Protein translocase subunit YajC
gi|492609716	119	12.4	9	PTS fructose transporter subunit IIC
gi|19704773	295	19.7	20	PTS system, fructose-specific IIABC component
gi|19705163	167	5.2	6	Short-chain fatty acids transporter
gi|19703712	82	39.5	15	Signal peptidase I
gi|19705203	119	20.3	12	Sugar transport ATP-binding protein
gi|19703496	293	35.8	17	3-oxoacyl-[acyl-carrier-protein] synthase
gi|19704546	126	15.5	10	Cell division protein FtsI
gi|19703805	113	4.3	3	Efflux pump component MtrF
gi|19704501	151	21.6	14	Galactose/methyl galaxtoside transporter ATP-binding protein
gi|19703566	134	11	9	Carbon starvation protein A
gi|19704710	85	12.3	4	Citrate-sodium symport
gi|496295757	152	37	18	Gtpase Der
gi|19704112	280	26.7	26	GTP-binding protein lepA
gi|19704050	184	25.5	12	Hypothetical protein FN0715
gi|19703521	666	76.9	52	Cell division inhibitor MinD
gi|19703515	86	20.5	13	GTP-binding protein EngA
gi|19703726	86	10.1	5	Hypothetical protein FN0384

TABLE S4. Periplasmic proteVins (15, 4.09%) identified in the proteome of F. nucleatum OMV

Accession number	Protein score	% Coverage	Number of peptide matches	Description
gi|19704500	1261	68.9	73	D-galactose-binding protein
gi|19704333	527	52	40	Dipeptide-binding protein FN0998
gi|19703738	3874	67.9	252	Dipeptide-binding protein FN0396
gi|19704855	380	37.5	35	Dipeptide-binding protein FN1523
gi|19704446	92	14.7	8	Dipeptide-binding protein FN1111
gi|19703717	1145	57.7	66	Iron(III)-binding protein
gi|19704730	92	8.1	4	Amino acid carrier protein AlsT
gi|19704522	91	16.3	4	Amino acid-binding protein
gi|19705117	76	12.6	3	Manganese-binding protein
gi|19704804	112	20.8	7	N-acetylneuraminate-binding protein
gi|19704836	528	37	34	Nickel-binding protein
gi|19704648	95	10.3	5	Oligopeptide-binding protein oppa FN1313

gi|19704973	176	17.8	10	Oligopeptide-binding protein oppa FN1652
gi|19704470	91	37.9	20	Phosphonates-binding protein
gi|19703953	225	47.4	22	Spermidine/putrescine-binding protein

TABLE S5. Outer membrane proteins (39, 10.62%) identified in the proteome of F. nucleatum OMV

Accession number	Protein score	% Coverage	Number of peptide matches	Description
gi|19705267	628	42	39	Hemin receptor
gi|19704535	581	78	44	Hypothetical protein FN1200
gi|19704858	8168	64.1	509	Hypothetical protein FN1526 (RadD)
gi|19704886	1739	35.4	119	Hypothetical protein FN1554
gi|19705337	3966	56.2	177	Hypothetical protein FN2047
gi|19703624	130	22.7	6	Lipoprotein 1
gi|492606366	2510	59.2	138	Membrane protein
gi|495968818	1032	30.4	115	Membrane protein
gi|492611696	6201	52.3	327	Membrane protein
gi|492656580	678	26	48	Outer membrane autotransporter barrel domain-containing protein
gi|19703678	920	76.2	50	Outer membrane porin F FN0335
gi|19703598	241	48.4	18	Outer membrane protein FN0253
gi|19704600	1264	36.1	40	Outer membrane protein FN1265
gi|19703736	495	53.3	51	Outer membrane protein FN0394
gi|19705216	2099	58	234	Outer membrane protein FN1911
gi|19704338	2548	76.2	117	Outer membrane protein P1 precursor FN1003
gi|19704608	1054	67.1	62	Outer membrane protein TolC
gi|496078626	3270	24.4	276	Outer membrane protein, partial
gi|492609940	157	23.4	8	Cell wall endopeptidase M23
gi|530296	21135	78.3	1456	Porin (FomA) FN1859
gi|19705025	114	17.9	13	Serine protease FN1074
gi|19705252	521	30.9	41	Serine protease FN1950
gi|19704758	5430	53.2	262	Serine protease FN1426
gi|492596693	841	12.3	73	Serine protease
gi|19703893	776	45.4	38	TraT complement resistance protein precursor
gi|492611516	2806	45.1	174	*Fusobacterium* outer membrane protein, partial
gi|19703727	127	28.1	11	Hypothetical protein FN0385

gi|19704200	639	71	54	Hypothetical protein FN0865
gi|492609727	205		22	*Fusobacterium* outer membrane protein
gi|496079010	1215	21	77	*Fusobacterium* outer membrane protein family
gi|19704402	366	60.8	24	Hypothetical protein FN1067
gi|19704070	2032	35.3	71	Cell surface protein FN0735
gi|492611840	1249	23.3	87	*Fusobacterium* outer membrane protein, partial
gi|19705141	4724	73.3	294	Hypothetical protein FN1836
gi|19703800	1207	68.5	92	Hypothetical protein FN0465
gi|19703945	937	49.8	121	Hypothetical protein FN0610
gi|19703599	2814	45.6	173	Hypothetical protein FN0254

TABLE S6. Proteins of unknown subcellular location (89, 24.25%) identified in the proteome of F. nucleatum OMV

Accession number	Protein score	% Coverage	Number of peptide matches	Description
gi|19704160	173	45.1	25	Cytoplasmic protein
gi|19703402	968	63.6	71	Fumarate reductase flavoprotein subunit
gi|492614404	4560	51.1	199	*Fusobacterium* outer membrane protein, partial
gi|19704587	270	49.6	18	34 kDa membrane antigen precursor
gi|19703581	184	40.7	14	ABC transporter substrate-binding protein
gi|66268805	87	35.1	5	Apoptosis inducing membrane protein
gi|19704593	453	46.2	33	C4-dicarboxylate-binding protein
gi|19703520	122	18.1	6	Cell division inhibitor minC
gi|19703522	112	47.5	11	Cell division inhibitor minE
gi|19704831	3558	50.9	141	Cell surface protein FN1499
gi|19704473	226	39.9	11	Cytoplasmic protein FN1138
gi|19703554	235	36	17	Cytoplasmic protein
gi|19704109	396	66.5	27	Cytoplasmic protein
gi|19705232	299	32.7	45	DEGV protein
gi|19703807	205	19.8	19	Flavodoxin flda
gi|496296672	1342	21.4	92	*Fusobacterium* outer membrane protein family, partial
gi|492611534	2863	35.7	157	*Fusobacterium* outer membrane protein, partial
gi|19705213	587	41.6	33	Glycerophosphodiester phosphodiesterase
gi|19703378	117	32.9	5	Hypothetical protein FN0026

gi|19703401	434	43.2	20	Hypothetical protein FN0049
gi|19703593	1034	68.8	56	Hypothetical protein FN0248
gi|19703609	1101	62	53	Hypothetical protein FN0264 (Fad A)
gi|19703625	268	27.2	15	Hypothetical protein FN0280
gi|19703694	388	70.8	20	Hypothetical protein FN0351
gi|19703713	206	23.9	12	Hypothetical protein FN0371
gi|19703732	103	52.6	10	Hypothetical protein FN0390
gi|19703749	917	69.5	54	Hypothetical protein FN0407
gi|19703892	130	26.2	12	Hypothetical protein FN0557
gi|19703936	106	50.4	15	Hypothetical protein FN0601
gi|19703972	96	45.3	13	Hypothetical protein FN0637
gi|19703990	141	50	12	Hypothetical protein FN0655
gi|19704024	459	62.1	29	Hypothetical protein FN0689
gi|19704053	170	14.7	5	Hypothetical protein FN0718
gi|19704066	243	63.8	30	Hypothetical protein FN0731
gi|19704156	693	45.1	71	Hypothetical protein FN0821
gi|19704167	282	74	11	Hypothetical protein FN0832
gi|19704240	254	65.3	24	Hypothetical protein FN0905
gi|19704251	1971	62.4	111	Hypothetical protein FN0916
gi|19704282	180	38.5	12	Hypothetical protein FN0947
gi|19704329	101	33.6	9	Hypothetical protein FN0994
gi|19704340	252	45.9	20	Hypothetical protein FN1005
gi|19704352	240	61.4	34	Hypothetical protein FN1017
gi|19704408	177	28	5	Hypothetical protein FN1073
gi|19704413	189	45.3	13	Hypothetical protein FN1078
gi|19704479	1240	67.1	100	Hypothetical protein FN1144
gi|19704488	183	32.1	5	Hypothetical protein FN1153
gi|19704548	253	33.3	16	Hypothetical protein FN1213
gi|19704588	1803	75.9	64	Hypothetical protein FN1253
gi|19704668	106	31.9	5	Hypothetical protein FN1333
gi|19704859	711	51.9	33	Hypothetical protein FN1527 (Fad I)
gi|19704861	81	45.5	2	Hypothetical protein FN1529
gi|19704892	129	25.1	5	Hypothetical protein FN1560
gi|19704968	2984	38.8	106	Hypothetical protein FN1647
gi|19705089	201	41.7	11	Hypothetical protein FN1784
gi|19705090	146	24.8	5	Hypothetical protein FN1785
gi|19705097	2107	73.6	74	Hypothetical protein FN1792
gi|19705112	639	62.1	31	Hypothetical protein FN1807
gi|19705130	313	51.7	21	Hypothetical protein FN1825

gi|19705140	84	23.1	3	Hypothetical protein FN1835
gi|19705157	172	40.5	11	Hypothetical protein FN1852
gi|19705198	4248	51.1	207	Hypothetical protein FN1893
gi|19705215	358	61.1	36	Hypothetical protein FN1910
gi|19705244	92	24.8	9	Hypothetical protein FN1939
gi|19705348	2281	37.2	119	Hypothetical protein FN2058
gi|19705411	541	51.7	40	Hypothetical protein FN2121
gi|523655036	1502	21	90	Hypothetical protein, partial
gi|19704460	170	51.9	14	LemA protein
gi|19705204	467	35.8	25	Lipoprotein 2
gi|492614725	554	50.1	32	Membrane protein
gi|496075624	1770	22.8	114	Membrane protein
gi|492610276	937	20.4	69	Membrane protein
gi|496075749	4243	39.5	238	Membrane protein
gi|496078982	4413	38.1	248	Membrane protein
gi|496070514	1312	18.7	84	Membrane protein
gi|492586863	1129	12.1	71	Membrane protein
gi|492647631	287	4.2	23	Membrane protein
gi|492564676	2158	15	187	Membrane protein
gi|492614450	8468	41.6	522	Membrane protein
gi|495977401	2768	19.3	257	Membrane protein
gi|19704915	100	24.9	5	Nitrogen fixation protein RNFG
gi|19703860	756	39.7	66	Penicillin-binding protein
gi|19705393	2071	84.1	106	RecAprotein
gi|19704409	120	26.7	8	Signal recognition particle receptor ftsy
gi|492611783	556	46.5	64	Stage II sporulation protein spoiid
gi|19704458	113	36.9	6	Thioredoxin-like protein FN1123
gi|492607145	206	27.2	15	Von Willebrand factor A
gi|19704354	314	24	11	3-hydroxybutyryl-coa dehydrogenase
gi|492620353	801		48	Galactoside ABC superfamily ATP binding cassette transporter, binding protein
gi|19704016	92	32.4	14	MarR family transcriptional regulator

Several proteases were identified in the OMV (Table S7). Gelatin zymography (Figure 1D) of the purified OMV and *F. nucleatum* shown in Figure 1C demonstrate abundant OMV-associated protease activity. In the image shown, there is no evidence of protease activity in whole *F. nucleatum*, however, activity could be detected if the bacteria were first subjected to a salt wash (PBS) and subsequently with KCl (0.5 M) to extract and concentrate cell surface-associated protease activities (Figure 1E). Throughout this procedure, the

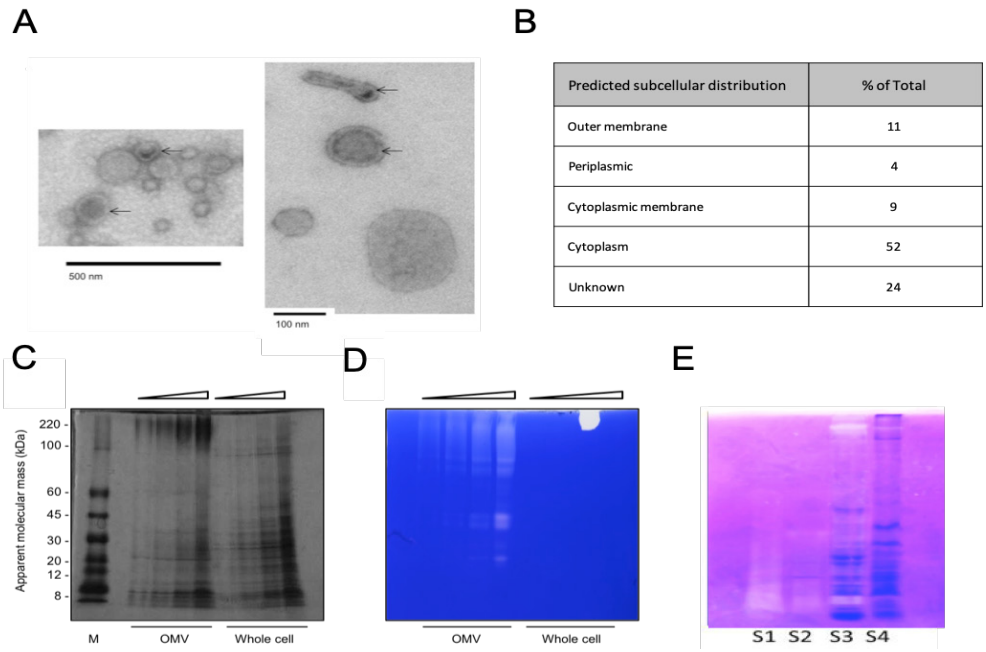

Predicted subcellular distribution	% of Total
Outer membrane	11
Periplasmic	4
Cytoplasmic membrane	9
Cytoplasm	52
Unknown	24

FIGURE 1. F. nucleatum OMV proteome and proteolytic activities. A: TEM images of F. nucleatum OMV indicating the presence of bi-layered O-IMVs (arrows). Scale bar: 100 nm and 500 nm. B: Summary of the predicted (pSortB) subcellular distribution of the 367 proteins identified by mass spectrometry C: Coomassie (G250) stained gradient (5–20%) SDS-PAGE gel of increasing amounts of OMV and F. nucleatum. D: Gelatin (0.1%) zymogram of the material shown in C. Zones of clearance indicate proteolysis. E: Gelatin (0.05 %) zymogram of subcellular fractionated proteolytic activity from F. nucleatum. S1: proteins recovered from a PBS-wash of whole cells. S2: 0.5 M KCL wash of PBS-treated cells. S3: cytoplasmic extract. S4: solubilized membrane extract. The apparent molecular mass markers are shown on the side of C (lane M).

TABLE S7. Proteases identified in the F. nucleatum OMV proteome

Accession number	Protein score	% Coverage	Number of peptide matches	Description	Subcellular location
gi|19704540	404	46.8	36	Protease FN1205	Cytosol
gi|19704606	121	13.3	14	Protease IV FN1271	Cytosol
gi|19705025	114	17.9	13	Serine protease FN1074	Outer Membrane
gi|19705252	521	30.9	41	Serine protease FN1950	Outer Membrane
gi|19704758	5430	53.2	262	Serine protease FN1426	Outer Membrane
gi|492596693	841	12.3	73	Serine protease	Outer Membrane
gi|19703623	94	17	5	Xaa-His dipeptidase	Cytosol
gi|49609940	157	23.4	8	Cell wall endopeptidase M23	Outer Membrane
gi|19703712	82	39.5	15	Signal peptidase	Cytosol

bacteria remained intact as judged by microscopy with no evidence of cellular debris (Figure S1). Additional protease activities were detected in the cytoplasmic and membrane fractions (Figure 1E). The substrate spectrum of the admixture of proteases was evaluated by co-incubating OMV, whole *F. nucleatum* or ion-exchange (Mono Q) fractionated (IEX) protease activity with various substrates (gelatin, azocasein, azoalbumin, E-cadherin). The IEX protease activities demonstrated differential abilities to degrade the non-specific chromogenic substrates azoalbumin and azocasein, with azocasein being preferentially degraded by the majority of protease active fractions (not shown). The ability of the whole bacteria (Fnn) and OMV to degrade E-cadherin was assessed also with evidence of proteolysis of E-cadherin by both *F. nucleatum* and OMV (Figure 2A).

Given the ability of both OMV and intact bacteria to degrade the adherens junctional molecule E-cadherin we investigated if both could modulate the epithelial barrier function (TEER) of T84 and Caco2 colonic cell monolayers. Both *F. nucleatum* and OMV reduced the TEER of Caco2 (Figure 2B) and T84 (Figure 2C) cells over time. The response of both cell lines to treatment with OMV and *F. nucleatum* differed, as indicated by the longer time to onset of the decrease in barrier integrity in Caco-2 compared with T84 cells.

4.2. OMV Induce Pro-inflammatory Cytokine Secretion from Colonic Epithelial Cells

Both OMV and whole *F. nucleatum* induced the expression of CXCL8 in a dose-dependent manner (Figure 3A and B) in SW480 cells and secretion of IL-8 by SW480, SW620, and T84 colonic cells at 6 and 24 h post-treatment was confirmed by ELISA (Figure 3C). Similarly, IL-8 secretion by SW480 cells was induced by *F. vincentii*, *F. polymorphum*, and their OMV (Figure 3D) and OMV-induced IL-8 secretion by SW480 cells was sustained over 72 h (Figure S2). Infection-induced secretion of IL-8 significantly reduced by the inhibitors SB203580 and PD98059 (Figure 3E), suggesting a role for the ERK mitogen-activated protein kinase (MAPK) and p38 MAPK pathways in OMV-mediated IL-8 expression.

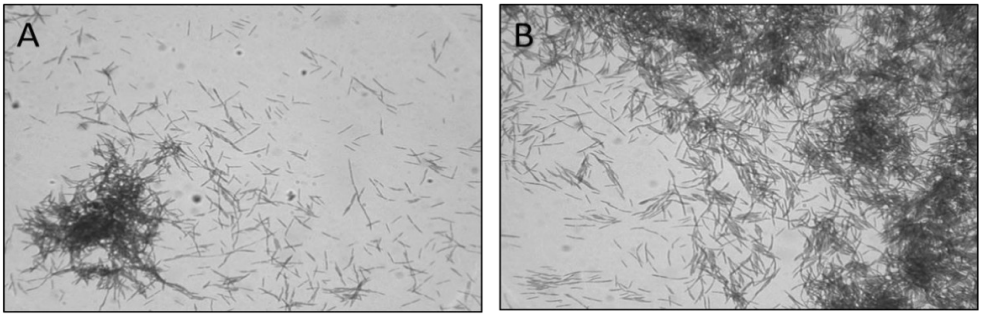

FIGURE S1. Gram stain of F. nucleatum recovered after extraction of protease activity by PBS and KCl wash. Panel A: F. nucleatum recovered after a PBS wash. Panel B: F. nucleatum recovered after a wash with PBS containing 0.5 M KCl. Magnification: oil immersion, 100×.

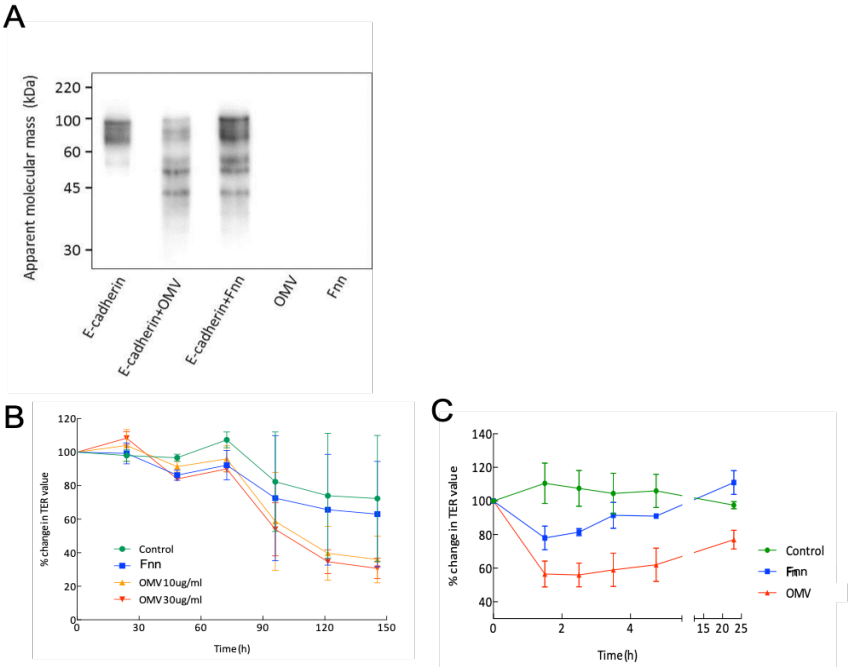

FIGURE 2. Effect of F. nucleatum and OMV on E-cadherin and the TEER of colonic cell monolayers. A: E-cadherin was co-incubated with OMV and F. nucleatum for 24 h prior to detecting products of E-cadherin degradation by Western blotting. B: Polarized and differentiated Caco2 and T84 cells (C) were treated with F. nucleatum and OMV once the cells reached a stable resistance (Time = 0) and the TEER monitored at regular intervals over 148 (B) or 24 h (C) for Caco2 and T84 cells, respectively.

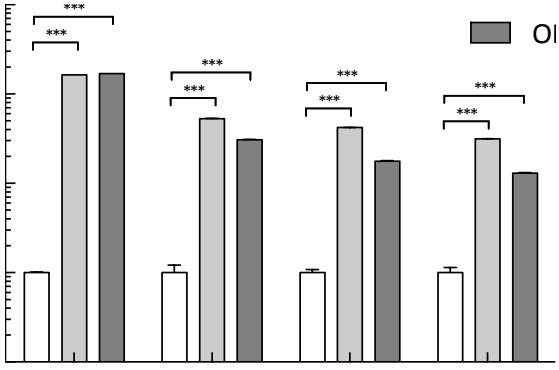

FIGURE S2. Time course of the effect of F. nucleatum and OMV in the induction of CXCL8 in SW-480 cells. SW-480 cells were treated with F. nucleatum (MOI 500:1) and OMV (30 µg/ml) for the times indicated and relative expression was determined by RT-PCR. *** = $p < 0.001$.

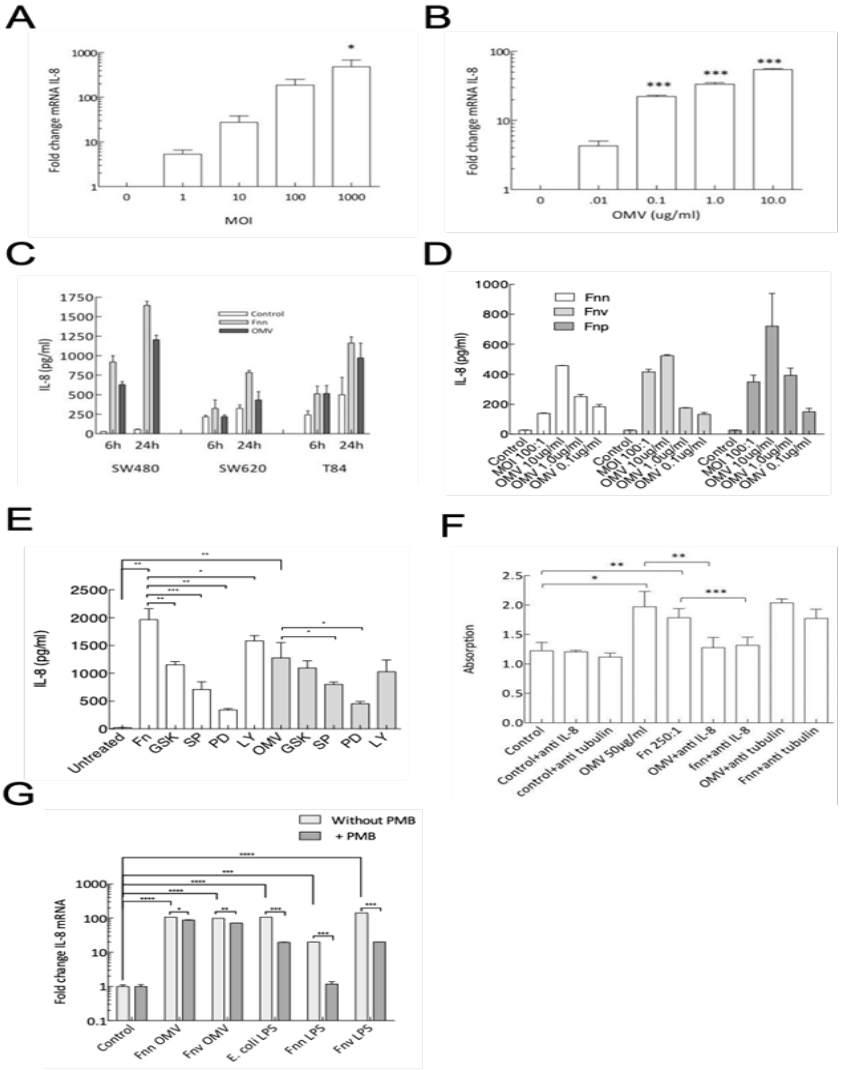

FIGURE 3. Effect of F. nucleatum and OMV on IL-8 gene and protein expression. Dose-dependent effect of F. nucleatum (A) and OMV (B) on CXCL8 expression in SW480 cells (n = 3). C: Time course (6/24 h) of IL-8 secretion by SW480, SW620, and T-48 cells in the absence or presence of F. nucleatum (MOI 200:1) or OMV (5 µg/ml). Secreted IL-8 was detected by ELISA (n = 2). D: The effect of co-incubation (24 h) of SW-480 cells with F. nucleatum (Fnn), F. vincentii (Fnv), and F. polymorphum (Fnp) (MOI: 100:1) and their OMV (0.1, 1, 10 µg/ml) on IL-8 secretion. IL-8 secretion was measured by ELISA (n = 2). E: Effect of metabolic inhibitors on F. nucleatum- (Fn, white bars, MOI 150:1) and OMV (10 µg/ml)-induced (grey bars) IL-8 secretion by SW-840 cells. The cells were treated with different inhibitors, GSK 690693 (GSK, 10 µM), SB203580 (SP, 50 µM), PD98059 (PD, 1 µM), and LY294002 (LY, 50 µM) for 2 h prior to the addition of bacteria or OMV and the incubation continued for an additional 4 h. F: IL-8 acts as an autocrine growth signal; SW480 cells were seeded in a 96-well plate until 20–30% confluent and then co-cultured alone or with F. nucleatum (MOI 250:1) or OMV (50 µg/ml) for 24 h. Where indicated, the cells were also treated after 24 h with monoclonal anti

FIGURE 3. *Continued*

IL-8 antibody (0.24 µg/ml) or monoclonal anti tubulin-α antibody (0.24 µg/ml), an isotype matched control, and the incubation continued for an additional 48 h after which time cell proliferation was assessed using Cell Titre One G: Contribution of F. nucleatum OMV LPS to IL-8 gene expression in SW-480 cells. The histogram illustrates the effect of polymyxin B (shaded bars) on CXCL8 expression in SW-480 cells treated with 10 ug/ml of F. nucleatum OMV, F. vincentii OMV, E. coli LPS, F. nucleatum LPS, and F. vincentii LPS for 4 h. The results are represented as the mean ± SEM (n = 3). * = $p < 0.05$, ** = $p < 0.01$, *** = $p < 0.001$, and **** = $p < 0.0001$.

Neither the PI3 kinase inhibitor LY294002 nor the Akt inhibitor GSK 690693 had a significant effect on IL-8 production by infected cells.

Both OMV- and *F. nucleatum*-induced IL-8 secreted by SW-480 cells appears to act in an autocrine-like manner to drive cell proliferation as this proliferative effect was significantly attenuated in the presence of a murine anti-human neutralizing IL-8 mAb whereas a matched isotype control mAb had no effect (Figure 3F). Interestingly, OMV-associated LPS only made a minor contribution to CXCL8 expression as demonstrated by the significant but minor effect of Polymyxin B on OMV-induced CXCL8 expression in SW-480 cells, unlike purified *F. nucleatum* LPS (Figure 3G) where Polymyxin B treatment reduced the expression to basal levels.

Both *F. nucleatum* and OMV induced expression of several other chemokines/cytokines and transcription factors *in vitro* including CXCL1, CXCL5, CCL20, TNF-α and IL-6 (Figure 4A), NF-kB1/2 (Figure 4B), and components of the Wnt pathway (Wnt 7A, 7B, 9A) (Figure 4C). In addition, the relative expression levels of Myc, SOCS3, SPHK1 and PGTS2 were increased on exposure of SW-480 cells to both *F. nucleatum* and OMV (Figure 4D). All these genes exhibit increased expression in individuals infected with moderate to high levels of *F. nucleatum* [5]. Finally, both *F. nucleatum* and OMV induced transient phosphorylation of STAT3 in SW-480 cells with an observed peak at 10 min, decreasing to control levels by 60 min (Figure 4E).

4.3. *F. nucleatum* and OMV Induce Morphological Changes and ZEB1 Gene and Protein Expression in Colonic Cells

Both *F. nucleatum* and OMV induced proliferation of SW480 cells as determined by monitoring wound closure in scratch wound assays and by direct colorimetric measurements of cell proliferation (not shown). Co-incubation of SW480 and SW620 cells with *F. nucleatum* and OMV, respectively, induced morphological changes with the cobblestone appearance of untreated SW480 cells (Figure 5A) becoming progressively more fibroblast-like after exposure to *F. nucleatum* with a clear reduction in the number of intracellular contacts. Occasionally, similar changes were observed when SW480 cells were treated with OMV but consistently observed when SW620 cells were treated with either *F. nucleatum* or OMV (not shown). As such changes occur when cells undergo epithelial mesenchymal transition (EMT) we determined their effects on nuclear

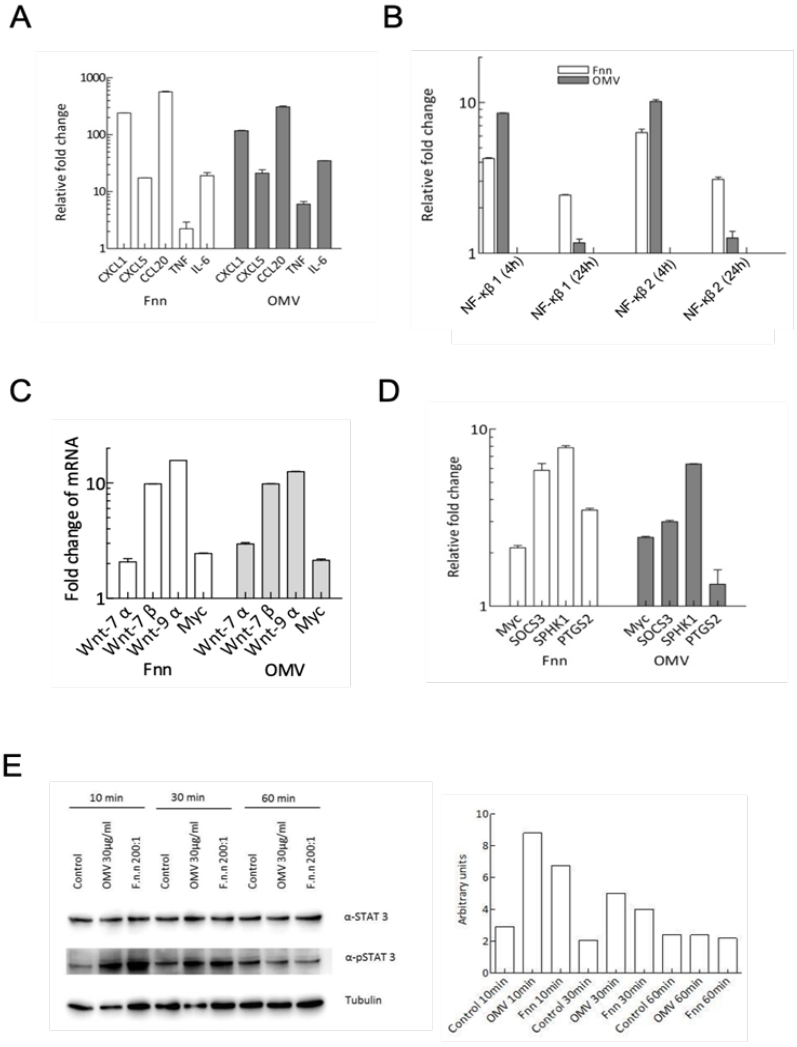

FIGURE 4. F. nucleatum and OMV induce pro-inflammatory transcription factors, cytokine/chermokines by colonic cells. A: F. nucleatum (MOI 100) and OMV (10 μg/ml) mediated induction of CXCL1, CXCL5, CCL20, TNF-α, IL-6 (A), NF-κβ1/2 h (B), Wnt-7 α, Wnt-7 β, Wnt-9 α(C) and Myc, SOCS3, SPHK1, PGTS2 (D). All co-incubations were for 4 h except in B, as indicated, and n = 2. E: Western blot of STAT3 phosphorylation (Y705) induced by F. nucleatum (MOI 200) and OMV (30 μg/ml)-treated (10–60 min) SW-480 cells. p-STAT-3 expression was normalized to total STAT-3 (histogram).

expression of ZEB1, a transcriptional repressor of CHD1 (E-cadherin), a hallmark of EMT. *F. nucleatum* stimulated ZEB1 nuclear expression in SW-480 cells as determined by immunofluorescence (Figure 5B) and qRT-PCR demonstrated a significant increase in *F. nucleatum* and OMV-induced ZEB1 expression (Figure 5C). Both the bacteria and their vesicles also stimulated ZEB1 accumulation in the nuclear fraction obtained from Caco2 (Figure 5D), SW-480, and SW-620 cells (not shown).

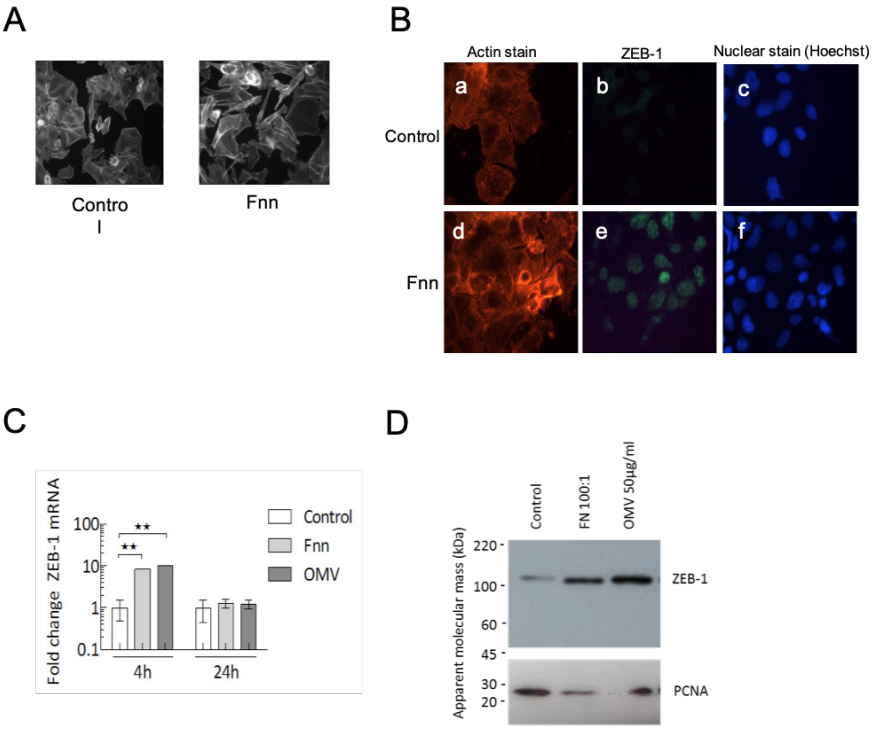

FIGURE 5. Effect of F. nucleatum and OMV on cellular morphology and ZEB1 expression in colonic cells. A: F. nucleatum (MOI 100) induce morphological changes in SW480 cells after co-incubation for 48 h. Cells were fixed and stained with phalloidin (magnification 40×). B: Immunofluorescence analysis of ZEB-1 nuclear expression in untreated (panel b) and F. nucleatum (MOI 100, 48 h) treated (panel e) SW480 cells. Also shown are the phalloidin (actin) (panels a, d) and Hoechst (panels c, f) stained cells (magnification 40×). C: ZEB1 mRNA expression in SW480 cells treated with F. nucleatum (Fnn, MOI 100) and OMV (10 µg/ml) for 4/24 h. D: Western blot showing ZEB1 expression in nuclear extracts of Caco2 cells treated with F. nucleatum (MOI 100) and OMV (50 µg/ml) for 48 h. PCNA was used as the nuclear fraction loading control (lower panel).

4.4. *F. nucleatum* and OMV Reduce CDH1 Protein and Gene Expression and Promote an EMT-like Genotype in Colonic Cells

Expression of CDH1 (transcript and protein) was down regulated in SW480 cells co-cultured with *F. nucleatum* and OMV as determined by immunofluorescence (Figure 6A), Western blotting (Figure 6B), and qRT-PCR (Figure 6C). In addition, mRNA of the mesenchymal markers CDH2 (N-cadherin), VIM (vimentin), ITGA5 (Integrin subunit α 5, and FN1 (fibronectin) was upregulated (Figure 6D) as was SNAI1/2/3 (Snail family transcriptional repressors) and TWIST (Twist family BHLH transcription factor 1) (Figure 6E). Finally, both OMV and *F. nucleatum* modulated MMP 1, 2, 3, 9, 10, and 13 expression (Figure 6F). Taken together, these data indicate that *F. nucleatum* and OMV can contribute to the process of transition towards a mesenchymal phenotype *in vitro*.

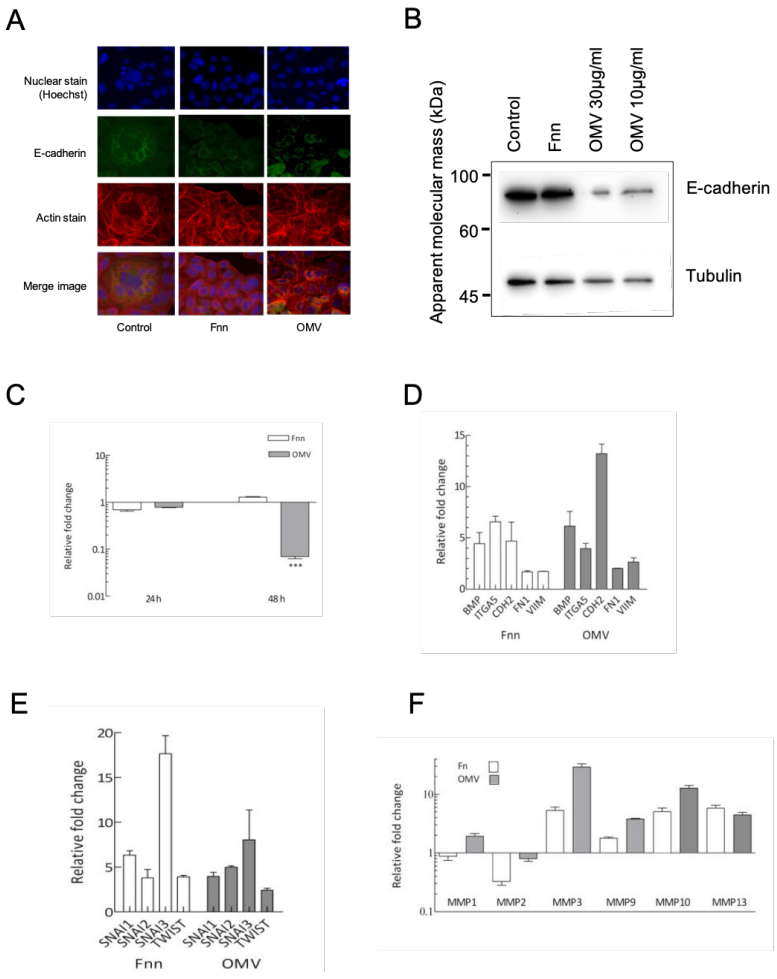

FIGURE 6. Effect of F. nucleatum and OMV on E-cadherin and EMT-marker expression. A: SW480 cells were treated with F. nucleatum (MOI 100:1) and OMV (50 µg/ml) for 24 h prior to detection of E-cadherin expression by immunofluorescence (green) (magnification 20×). B: Western blot showing reduced expression of E-cadherin in F. nucleatum (MOI 100) and OMV (10, 30 µg/ml)-treated cells. C: RT-PCR analysis of CDH1 expression in SW480 cells treated with F. nucleatum (MOI 200) and OMV (20 µg/ml) for 24–48 h ($n = 3$; $p < 0.001$) D: Expression of mesenchymal marker genes (BMP, ITGA5, CDH2, FN1, VIM) in SW480 cells induced by F. nucleatum and OMV treatment (4 h, $n = 2$). E: Expression of SNAI3 and TWIST in SW480 cells co-cultured (4 h) with F. nucleatum and OMV ($n = 2$). F: F. nucleatum and OMV modulate MMP (1, 2, 3, 9, 10, and 13) expression in SW480 cells after co-culture for 4 h ($n = 2$).

5. Discussion

This study evaluated the ability of OMV from *F. nucleatum* to modulate cellular responses in colonic cells with respect to factors involved in inflammation and disease in the context of CRC. *F. nucleatum* is emerging as a pathogen of medical importance due to its significant

association with CRC, and OMV from bacterial pathogens are known to promote disease progression. Thus, OMV were recovered from a sequenced (and invasive) strain of *F. nucleatum* (ATCC 25586) and the protein composition determined by mass spectrometry, resulting in the identification of 367 proteins. The presence of cytoplasmic proteins in the OMV preparation likely arises due to the presence of outer–inner membrane vesicles [21].

The *F. nucleatum* OMV proteome contains proteins known to be associated with pathogenesis [22] including the important adhesin FadA (FN0264) [6], and two others responsible for mediating multi-species co-aggregation, RadD (FN1526), and FomA (FN1859). RadD also mediates cell death in human lymphocytes [23]. In addition, active proteases were identified in the OMV which are capable of degrading host proteins.

Two other reports identified serine protease activity in *F. nucleatum* OMV reportedly capable of degrading IgA, fibronectin, and collagen [24–25]. Here we demonstrate the ability of OMV to degrade E-cadherin. Similar activity was observed with whole bacteria or with proteases partially purified from whole *F. nucleatum*, although the rates of degradation were slow when compared with other bacterial proteases with similar substrate specificity (e.g., HtrA from *H. pylori* [26]). Furthermore, OMV and *F. nucleatum* reduced the barrier integrity of colonic epithelial cell monolayers (T84 and Caco2) with OMV reducing the TEER more completely than intact *F. nucleatum*, suggesting that OMV can more efficiently transport proteolytic activity to the host cells. Such OMV-associated protease activity can damage host tissue [27–28] and disrupt intestinal barrier function and integrity [25]. Attempts were made to inhibit the *F. nucleatum* and OMV protease activity using a pan-protease inhibitor cocktail was unsuccessful as the inhibitors alone also modulated the barrier integrity. Additional attempts were made to pre-incubate OMV with the inhibitors followed by ultra-centrifugal washing prior to use but this approach led to significant loss of OMV.

Vesiculation is conserved biological process of gram-negative bacteria and has been shown to occur *in vivo* [29]. Analysis of OMV composition has provided evidence for selective enrichment of specific molecules, including proteases, in OMV from a variety of bacteria [30–35] and may also be the case in *F. nucleatum* OMV as judged by zymography. As OMV are not restricted to the niche occupied by the parental bacterium, they are a means for delivering effectors molecules in concentrated form to host cells [36–37] where they elicit potent inflammatory and other effects [33,38–41]. Vesicles are also involved in intercellular communication [42], horizontal transfer of virulence factors to eukaryotic cells and antibiotic resistance between bacteria [35,43]. In addition to protecting the bacteria from the host's innate immune response [44–45] they have been implicated in the pathogenesis of a broad range of infectious diseases, including periodontitis [33], gastritis [29,38], Crohn disease [40], salpingitis [46], meningitis [47–48], sepsis [49], and cardiovascular [50] and pulmonary disease [37].

In addition, OMVs are highly immunogenic and are considered to enhance pathogenicity by triggering the release of pro-inflammatory and immune regulatory cytokines, inducing neutrophil migration and recruitment and disrupting tight junctions in epithelial cell mono-layers [28,51]. Both *F. nucleatum* and OMV elicit potent pro-inflammatory responses in colonic epithelial cells as shown by increased transcript or protein abundance of CXCL1, CXCL5, CXCL8, CCL20, IL6, TFNα, NFkB1 (p105/p50),

and NFkB2 (p100/p50). Several of these and other inflammatory cytokine/chemokines are dysregulated in adenomas [52] which negatively influences patient prognosis [53]. NF-kB can be activated by >150 stimuli and >150 genes are expressed on its activation [54–55]. Many of these genes encode proteins known to be essential for invasion and metastasis including adhesion molecules, MMPs, serine proteases, as well as pro-inflammatory cytokines and chemokines (e.g., TNFα, IL-1a, IL-6, CXCL8) which are associated with tumor development and progression in humans and mice [56–57]. Several studies have demonstrated the pro-inflammatory potential of *F. nucleatum* as evidenced by its ability to promote pro-inflammatory cytokine secretion from a variety of colonic/oral epithelial cells [58–60] and immune cells [61] and various Fusobacterial proteins can elicit this response including the major outer membrane FomA [62], the heat shock protein GroEL [63], and peptidoglycan [64], the former two being identified in the OMV proteome. Interestingly, although we have shown that *F. nucleatum*LPS induces CXCL8, the OMV-bound LPS appears to make little contribution to CXCL8 secretion by colonic cells suggesting that other constituents in the OMV are responsible for this activity.

Both *F. nucleatum* and OMV induced an EMT-like phenotype and genotype in colonic cells in vitro. In the presence of *F. nucleatum* and OMV, translocation of the transcriptional repressor ZEB1 to the nucleus was induced in colonic cells. Evidence of a mesenchymal genotype emerged upon treatment of SW-480 cells with *F. nucleatum* and OMV, as shown by the increased transcription of the mesenchymal markers CDH2 (N-cadherin), VIM (vimentin), ITGA5 (integrin subunit α5), FN1 (fibronectin), MMP3, MMP9, MMP10, and MMP13. Downregulation of E-cadherin is one of the essential initial events for EMT and is considered a hallmark of this process [65]. Both *F. nucleatum* and OMV also increased expression of the transcriptional repressors SNAI1, SNAI2, SNAI3, and TWIST with all implicated in carcinogenesis: for example, SNAI1 represses transcription of CDH1; SNAI2 induces the first phase of EMT, including desmosome dissociation, cell spreading, and initiation of cell separation [66–67]. N-cadherin is expressed by many tumor types and is associated with poor prognosis [68–69] and likewise with VIM [70–71] and FN1 [72–74]. Furthermore, both OMV and *F. nucleatum* activated STAT3 in colonic cells, a transcription factor known to be activated in various malignancies, including colon cancer [75]. Phosphorylated STAT3 regulates transcription of target genes (e.g., c-Myc) involved in promoting cell survival, proliferation, migration, and oncogenic transformation [76].

Among the E-cadherin repressors, ZEB1 is the most potent [77–78]. ZEB1 also represses regulators of epithelial differentiation, including cell polarity proteins, tight junctional proteins, desmosomes and gap junctional proteins [77] and has a role as a positive regulator of mesenchymal genes [79–80] and is implicated in aggressive cancers [81–82]. In colon cancer, ZEB1 was observed upregulated at the tumor–host interface and was accompanied by epithelial dedifferentiation and tumor cell invasion [77] in addition repressing the expression of laminin genes and this transient loss of a basement membrane component correlated with increased metastasis and poor patient survival [83].

EMT initiation (and ZEB1) is influenced by multiple signaling pathways including TGFb, RTKs, Wnt, IL-6/STAT3, NOTCH and TNF-α and control of expression by ZEB1 is cell and context dependent [79]. Microbe-induced EMT is now recognized to be elicited

by several pathogens including *H. pylori* [84–85], *K. pneumoniae* [86], *M. tuberculosis* [87], *P. gingivalis* [88], *C. rodentium* [89], *S. typhimurium* [90], and *P. aeruginosa* [91].

6. Conclusion

These data demonstrate the potential for OMV from *F. nucleatum* to elicit phenotypic and genotypic modifications to colonic cells consistent with progression towards a more tumorigenic milieu. Further studies evaluating the pathogenic potential of these OMV *in vivo* are warranted.

Acknowledgement

The author thanks the Ministry of Higher Education in Saudi Arabia for granting a scholarship to continue the study in Ireland and also his research supervisor Dr. Henry Windle to complete this study.

References

1. Vogelstein B. Cancer genome landscapes. *Science*. 2013; 339(6127), 1546–1558.
2. Garrett WS. Cancer and the microbiota. *Science*. 2015; 348(6230), 80–86.
3. Wang T. Structural segregation of gut microbiota between colorectal cancer patients and healthy volunteers. *The ISME Journal*. 2012; 6(2), 320–329.
4. Warren RL. Co-occurrence of anaerobic bacteria in colorectal carcinomas. *Microbiome*. 2013; 1(1), 16.
5. Kostic AD. *Fusobacterium nucleatum* potentiates intestinal tumorigenesis and modulates the tumor-immune microenvironment. *Cell Host & Microbe*. 2013; 14(2), 207–215.
6. Rubinstein MR. *Fusobacterium nucleatum* promotes colorectal carcinogenesis by modulating E-cadherin/β-catenin signaling via its FadA adhesin. *Cell Host & Microbe*. 2013; 14(2), 195–206.
7. Castellarin M. *Fusobacterium nucleatum* infection is prevalent in human colorectal carcinoma. *Genome Research*. 2012; 22(2), 299–306.
8. Kostic AD. Genomic analysis identifies association of Fusobacterium with colorectal carcinoma. *Genome Research*. 2012; 22(2), 292–298.
9. Flanagan L. *Fusobacterium nucleatum* associates with stages of colorectal neoplasia development, colorectal cancer and disease outcome. *European Journal of Clinical Microbiology & Infectious Diseases*. 2014; 33(8), 1381–1390.
10. Li YY. Association of *Fusobacterium nucleatum* infection with colorectal cancer in Chinese patients. *World Journal of Gastroenterology*. 2016; 22(11), 3227.
11. Wei Z. Could gut microbiota serve as prognostic biomarker associated with colorectal cancer patients' survival? A pilot study on relevant mechanism. *Oncotarget*. 2016; 7(29), 46158.
12. Gur C. Binding of the Fap2 protein of *Fusobacterium nucleatum* to human inhibitory receptor TIGIT protects tumors from immune cell attack. *Immunity*. 2015; 42(2), 344–355.
13. Suehiro Y. Highly sensitive stool DNA testing of *Fusobacterium nucleatum* as a marker for detection of colorectal tumors in a Japanese population. *Annals of Clinical Biochemistry*. 2017; 54(1), 86–91.

14. Han YW. Identification and characterization of a novel adhesin unique to oral fusobacteria. *Journal of Bacteriology*. 2005; 187(15), 5330–5340.
15. Horiuchi A. Synergistic biofilm formation by *Parvimonas micra* and *Fusobacterium nucleatum*. *Anaerobe*. 2019, 102100.
16. Gendron R, Plamondon P, Grenier D. Binding of pro-matrix metalloproteinase 9 by *Fusobacterium nucleatum* subsp. nucleatum as a mechanism to promote the invasion of a reconstituted basement membrane. *Infection and Immunity*. 2004; 72(10), 6160–6163.
17. Leibovitz A. Classification of human colorectal adenocarcinoma cell lines. *Cancer Research*. 1976; 36(12), 4562–4569.
18. Mullaney E. Proteomic and functional characterization of the outer membrane vesicles from the gastric pathogen *Helicobacter pylori*. *PROTEOMICS–Clinical Applications*. 2009; 3(7), 785–796.
19. Eugene CY, Hackett M. Rapid isolation method for lipopolysaccharide and lipid A from gram-negative bacteria. *Analyst*. 2000; 125(4), 651–656.
20. Tsai CM, Frasch CE. A sensitive silver stain for detecting lipopolysaccharides in polyacrylamide gels. *Analytical Biochemistry*. 1982; 119(1), 115–119.
21. Pérez-Cruz C. Outer-inner membrane vesicles naturally secreted by gram-negative pathogenic bacteria. *PLoS One*. 2015; 10(1), e0116896.
22. Lee J, Kim OY, Gho YS. Proteomic profiling of Gram-negative bacterial outer membrane vesicles: current perspectives. *PROTEOMICS–Clinical Applications*. 2016; 10(9–10), 897–909.
23. Kaplan CW. *Fusobacterium nucleatum* outer membrane proteins Fap2 and RadD induce cell death in human lymphocytes. *Infection and Immunity*. 2010; 78(11), 4773–4778.
24. Bachrach G. Identification of a *Fusobacterium nucleatum* 65 kDa serine protease. *Oral Microbiology and Immunology*. 2004; 19(3), 155–159.
25. Doron L. Identification and characterization of fusolisin, the *Fusobacterium nucleatum* autotransporter serine protease. *PLoS One*. 2014; 9(10), e111329.
26. Hoy B. Distinct roles of secreted HtrA proteases from gram-negative pathogens in cleaving the junctional protein and tumor suppressor E-cadherin. *Journal of Biological Chemistry*. 2012; 287(13), 10115–10120.
27. Nakao R. Effect of *Porphyromonas gingivalis* outer membrane vesicles on gingipain-mediated detachment of cultured oral epithelial cells and immune responses. *Microbes and Infection*. 2014; 16(1), 6–16.
28. Chi B, Qi M, Kuramitsu HK. Role of dentilisin in *Treponema denticola* epithelial cell layer penetration. *Research in Microbiology*. 2003; 154(9), 637–643.
29. Fiocca R. Release of *Helicobacter pylori* vacuolating cytotoxin by both a specific secretion pathway and budding of outer membrane vesicles. Uptake of released toxin and vesicles by gastric epithelium. *The Journal of Pathology*. 1999; 188(2), 220–226.
30. Kato S, Kowashi Y, Demuth DR. Outer membrane-like vesicles secreted by *Actinobacillus actinomycetemcomitans* are enriched in leukotoxin. *Microbial Pathogenesis*. 2002; 32(1), 1–13.
31. Elhenawy W, Debelyy MO, Feldman MF. Preferential packing of acidic glycosidases and proteases into Bacteroides outer membrane vesicles. *MBio*. 2014; 5(2), e00909– e00914.
32. Haurat MF. Selective sorting of cargo proteins into bacterial membrane vesicles. *Journal of Biological Chemistry*. 2011; 286(2), 1269–1276.
33. Veith PD. *Porphyromonas gingivalis* outer membrane vesicles exclusively contain outer membrane and periplasmic proteins and carry a cargo enriched with virulence factors. *Journal of Proteome Research*. 2014; 13(5), 2420–2432.
34. Bonnington K, Kuehn M. Protein selection and export via outer membrane vesicles. *Biochimica et Biophysica Acta (BBA)-Molecular Cell Research*. 2014; 1843(8), 1612–1619.

35. Kulp A, Kuehn J. Biological functions and biogenesis of secreted bacterial outer membrane vesicles. *Annual Review of Microbiology*. 2010; 64, 163–184.
36. Manning AJ, Kuehn MJ. Functional advantages conferred by extracellular prokaryotic membrane vesicles. *Journal of Molecular Microbiology and Biotechnology*. 2013; 23(1–2), 131–141.
37. Bomberger JM. Long-distance delivery of bacterial virulence factors by *Pseudomonas aeruginosa* outer membrane vesicles. PLoS Pathogens. 2009; 5(4), e1000382.
38. Kaparakis M. Bacterial membrane vesicles deliver peptidoglycan to NOD1 in epithelial cells. *Cellular Microbiology*. 2010; 12(3), 372–385.
39. Irving AT. The immune receptor NOD1 and kinase RIP2 interact with bacterial peptidoglycan on early endosomes to promote autophagy and inflammatory signaling. *Cell Host & Microbe*. 2014; 15(5), 623–635.
40. Rolhion N, Abnormally expressed ER stress response chaperone Gp96 in CD favours adherent-invasive *Escherichia coli* invasion. *Gut*. 2010; 59(10), 1355–1362.
41. Ellis TN, Kuehn MJ. Virulence and immunomodulatory roles of bacterial outer membrane vesicles. *Microbiology and Molecular Biology Reviews*. 2010; 74(1), 81–94.
42. Mashburn LM, Whiteley M. Membrane vesicles traffic signals and facilitate group activities in a prokaryote. *Nature*. 2005; 437(7057), 422.
43. Rompikuntal PK. Perinuclear localization of internalized outer membrane vesicles carrying active cytolethal distending toxin from *Aggregatibacter actinomycetemcomitans*. *Infection and Immunity*. 2012; 80(1), 31–42.
44. Grenier D, Belanger M. Protective effect of *Porphyromonas gingivalis* outer membrane vesicles against bactericidal activity of human serum. *Infection and Immunity*. 1991; 59(9), 3004–3008.
45. Manning AJ, Kuehn MJ. Contribution of bacterial outer membrane vesicles to innate bacterial defense. *BMC Microbiology*. 2011; 11(1), 258.
46. Gregg CR. Toxic activity of purified lipopolysaccharide of *Neisseria gonorrhoeae* for human fallopian tube mucosa. *Journal of Infectious Diseases*. 1981; 143(3), 432–439.
47. Stephens DS. Pili and outer membrane appendages on *Neisseria meningitidis* in the cerebrospinal fluid of an infant. *Journal of Infectious Diseases*. 1982; 146(4), 568.
48. Namork E, Brandtzaeg P. Fatal meningococcal septicaemia with "blebbing" meningococcus. *The Lancet*. 2002; 360(9347), 1741.
49. Shah B. Circulating bacterial membrane vesicles cause sepsis in rats. *Shock*. 2012; 37(6), 621–628.
50. Kuramitsu HK. Role for periodontal bacteria in cardiovascular diseases. *Annals of Periodontology*. 2001; 6(1), 41–47.
51. Sharpe SW, Kuehn MJ, Mason KM. Elicitation of epithelial cell-derived immune effectors by outer membrane vesicles of nontypeable *Haemophilus influenzae*. *Infection and Immunity*. 2011; 79(11), 4361–4369.
52. McLean MH. The inflammatory microenvironment in colorectal neoplasia. *PLoS One*. 2011; 6(1), e15366.
53. Galon J. Type, density, and location of immune cells within human colorectal tumors predict clinical outcome. *Science*. 2006; 313(5795), 1960–1964.
54. Pahl HL. Activators and target genes of Rel/NF-κB transcription factors. *Oncogene*. 1999; 18(49), 6853.
55. Bhatt D, Ghosh S. Regulation of the NF-κB-mediated transcription of inflammatory genes. *Frontiers in Immunology*. 2014; 5, 71.
56. Balkwill F, Mantovani A. Inflammation and cancer: back to Virchow? *The Lancet*. 2001; 357(9255), 539–545.

57. Balkwill FR. The chemokine system and cancer. *The Journal of Pathology*. 2012; 226(2), 148–157.
58. Tang B. *Fusobacterium nucleatum*-induced impairment of autophagic flux enhances the expression of proinflammatory cytokines via ROS in Caco-2 cells. *PLoS One*. 2016; 11(11), e0165701.
59. Kang MS. Effects of methyl gallate and gallic acid on the production of inflammatory mediators interleukin-6 and interleukin-8 by oral epithelial cells stimulated with *Fusobacterium nucleatum*. *The Journal of Microbiology*. 2009; 47(6), 760–767.
60. Stathopoulou PG. Epithelial cell pro-inflammatory cytokine response differs across dental plaque bacterial species. *Journal of Clinical Periodontology*. 2010; 37(1), 24–29.
61. Kurgan Ş. Strain-specific impact of *Fusobacterium nucleatum* on neutrophil function. *Journal of Periodontology*. 2017; 88(4), 380–389.
62. Toussi DN, Liu X, Massari P. The FomA porin from *Fusobacterium nucleatum* is a toll-like receptor 2 agonist with immune adjuvant activity. *Clinical and Vaccine Immunology*. 2012; 19(7), 1093–1101.
63. Lee HR. *Fusobacterium nucleatum* GroEL induces risk factors of atherosclerosis in human microvascular endothelial cells and ApoE−/− mice. *Molecular Oral Microbiology*. 2012; 27(2), 109–123.
64. Okugawa T. NOD1 and NOD2 mediate sensing of periodontal pathogens. *Journal of Dental Research*. 2010; 89(2), 186–191.
65. Huber MA, Kraut N, Beug H. Molecular requirements for epithelial–mesenchymal transition during tumor progression. *Current Opinion in Cell Biology*. 2005; 17(5), 548–558.
66. Peinado H. Snail and E47 repressors of E-cadherin induce distinct invasive and angiogenic properties in vivo. *Journal of Cell Science*. 2004; 117(13), 2827–2839.
67. De Craene B. The transcription factor snail induces tumor cell invasion through modulation of the epithelial cell differentiation program. *Cancer Research*. 2005; 65(14), 6237–6244.
68. Blaschuk OW. N-cadherin antagonists as oncology therapeutics. *Philosophical Transactions of the Royal Society B: Biological Sciences*. 2015; 370(1661), 20140039.
69. Ye Z. Expression of lncRNA-CCAT1, E-cadherin and N-cadherin in colorectal cancer and its clinical significance. *International Journal of Clinical and Experimental Medicine*. 2015; 8(3), 3707.
70. Satelli A, Li S. Vimentin in cancer and its potential as a molecular target for cancer therapy. *Cellular and Molecular Life Sciences*. 2011; 68(18), 3033–3046.
71. Ivaska J. Vimentin: central hub in EMT induction? *Small GTPases*. 2011; 2(1), 1436–1448.
72. Bates RC, Mercurio A. The epithelial-mesenchymal transition (EMT) and colorectal cancer progression. *Cancer Biology & Therapy*. 2005; 4(4), 371–376.
73. Cantor D. Overexpression of αvβ6 integrin alters the colorectal cancer cell proteome in favor of elevated proliferation and a switching in cellular adhesion that increases invasion. *Journal of Proteome Research*. 2013; 12(6), 2477–2490.
74. Takamura M. Reduced expression of liver–intestine cadherin is associated with progression and lymph node metastasis of human colorectal carcinoma. *Cancer Letters*. 2004; 212(2), 253–259.
75. Zhang G, Yang W, Chen Z. Upregulated STAT3 and RhoA signaling in colorectal cancer (CRC) regulate the invasion and migration of CRC cells. *European Review for Medical and Pharmacological Sciences*. 2016; 20(10), 2028–2037.
76. Yu H. Revisiting STAT3 signalling in cancer: new and unexpected biological functions. *Nature Reviews Cancer*. 2014, 14(11), 736.
77. Aigner K. The transcription factor ZEB1 (δEF1) promotes tumour cell dedifferentiation by repressing master regulators of epithelial polarity. *Oncogene*. 2007; 26(49), 6979.

78. Takeyama Y. Knockdown of ZEB1, a master epithelial-to-mesenchymal transition (EMT) gene, suppresses anchorage-independent cell growth of lung cancer cells. *Cancer Letters*. 2010; 296(2), 216–224.
79. Vandewalle C, Van Roy F, Berx G. The role of the ZEB family of transcription factors in development and disease. Cellular and molecular life sciences. 2009, 66 (5), pp. 773-787.
80. Lamouille S, Xu J, Derynck R. Molecular mechanisms of epithelial–mesenchymal transition. *Nature Reviews Molecular Cell Biology*. 2014; 15(3), 178.
81. Sánchez-Tilló E. EMT-activating transcription factors in cancer: beyond EMT and tumor invasiveness. *Cellular and Molecular Life Sciences*. 2012; 69(20), 3429–3456.
82. Spoelstra NS. The transcription factor ZEB1 is aberrantly expressed in aggressive uterine cancers. *Cancer Research*. 2006; 66(7), 3893–3902.
83. Spaderna S. A transient, EMT-linked loss of basement membranes indicates metastasis and poor survival in colorectal cancer. *Gastroenterology*. 2006; 131(3), 830–840.
84. Choi YJ. *Helicobacter pylori*-induced epithelial-mesenchymal transition, a potential role of gastric cancer initiation and an emergence of stem cells. *Carcinogenesis*. 2015; 36(5), 553–563.
85. Sougleri IS. *Helicobacter pylori* CagA protein induces factors involved in the epithelial to mesenchymal transition (EMT) in infected gastric epithelial cells in an EPIYA-phosphorylation-dependent manner. *The FEBS Journal*. 2016; 283(2), 206–220.
86. Leone L. *Klebsiella pneumoniae* is able to trigger epithelial-mesenchymal transition process in cultured airway epithelial cells. *PLoS One*. 2016; 11(1), e0146365.
87. Gupta PK. *Mycobacterium tuberculosis* H37Rv infected THP-1 cells induce epithelial mesenchymal transition (EMT) in lung adenocarcinoma epithelial cell line (A549). *Cellular Immunology*. 2016; 300, 33–40.
88. Sztukowska MN. *Porphyromonas gingivalis* initiates a mesenchymal-like transition through ZEB1 in gingival epithelial cells. *Cellular Microbiology*. 2016; 18(6), 844–858.
89. Chandrakesan A. Utility of a bacterial infection model to study epithelial–mesenchymal transition, mesenchymal–epithelial transition or tumorigenesis. *Oncogene*. 2014; 33(20), 2639.
90. Tahoun A. Salmonella transforms follicle-associated epithelial cells into M cells to promote intestinal invasion. *Cell Host & Microbe*. 2012; 12(5), 645–656.
91. Borthwick L. *Pseudomonas aeruginosa* accentuates epithelial-to-mesenchymal transition in the airway. *European Respiratory Journal*. 2011; 37(5), 1237–1247.